

# Activation and Inhibition of the Mg-Ca-ATPase from *E. coli* by $Mg^{2+}$ and $Ca^{2+}$

Jan Ahlers and Theodor Günther

Zentralinstitut für Biochemie und Biophysik, Freie Universität Berlin

(Z. Naturforsch. 30c, 412–416 [1975]; received January 7, 1975)

Mg-Ca-ATPase, *E. coli*, Activation, Inhibition

MgATP or CaATP is the substrate of the Mg-Ca-ATPase. At low  $Mg^{2+}$ - or  $Ca^{2+}$ -concentrations the ATPase is activated by  $Mg^{2+}$  or  $Ca^{2+}$ , the activator being essential for activity. At higher  $Mg^{2+}$ - or  $Ca^{2+}$ -concentrations the Mg-Ca-ATPase is inhibited competitively. Thus the real  $K_m$  is smaller than reported in the literature.  $H^+$  competes with  $Mg^{2+}$  or  $Ca^{2+}$  for the metal binding sites.

## Introduction

The Mg-Ca-ATPase of *E. coli* is involved in oxidative phosphorylation and in ATP-dependent membrane functions<sup>1–3</sup> (active transport of amino acids and  $K^+$  under anaerobic conditions, ATP-driven transhydrogenase). The enzymatic properties of the Mg-Ca-ATPase were extensively studied (for literature see ref. 4).

However, the effect of the single components of the substrate ( $Mg^{2+}$ ,  $Ca^{2+}$ , ATP, MgATP, CaATP) on *E. coli* ATPase activity is not defined. For analysing these complex relations we examined the MgATP-dependence at constant pMg values and the pMg dependence at constant MgATP-concentrations.

## Materials and Methods

**Symbols and Abbreviations:** S = substrate (MgATP, CaATP); P = product(s);  $[Me^{2+}]$  = concentration of free metal ions ( $Mg^{2+}$ ,  $Ca^{2+}$ );  $[Me^{2+}]_t$ ,  $[ATP]_t$  = total concentrations; pMe = negative logarithm of metal ion concentration.

### Preparation of the Mg-Ca-dependent ATPase

*E. coli* strain B 163 was cultured as described by Günther and Dorn<sup>5</sup>. The ATPase was prepared as described by Evans<sup>6</sup>.

### Determination of enzyme activity

The enzyme activity was tested at 37 °C in 10.0 ml 100 mM Tris buffer, titrated with 2 N HCl to pH 7.5, 8.2 and 9.1. After 10 min preincubation with  $MgCl_2$  or  $CaCl_2$  the reaction was started by

Requests for reprints should be sent to Dr. Jan Ahlers, Zentralinstitut für Biochemie/Biophysik, D-1000 Berlin 33, Arnimallee 22.

adding ATP. Total ATP-concentrations amounted to 0.05, 0.10, 0.15, 0.20, 0.25, 0.30, 0.40, 0.50, 1.00 and 1.50 mM. To each  $[ATP]_t$  the following  $[Mg^{2+}]_t$  or  $[Ca^{2+}]_t$  were added: 0.02, 0.05, 0.10, 0.20, 0.30, 0.50, 1.00, 2.00 mM.

The reaction was followed by continuously measuring the release of inorganic phosphate<sup>7,8</sup>, as described by Ahlers<sup>9</sup>. In order to dissolve the membranes, 6% sodium dodecylsulfate was added continuously together with TCA. Care was taken to ensure that the hydrolysis of the substrate amounted to 5% but never exceeded 10% of the total substrate concentration. So the measurements were always being made in the area of linearity and under steady-state conditions.

Protein was determined by the method of Lowry *et al.*<sup>10</sup> using bovine serum albumin as a standard. Calculation of  $[MgATP]$ ,  $[CaATP]$ ,  $[ATP]$ ,  $[Ca^{2+}]$  and  $[Mg^{2+}]$

From the 80 mixtures of  $Me^{2+}$  and ATP at each pH the resulting concentrations of MeATP were calculated using the following equation:

$$[MeATP] = \frac{[Me^{2+}]_t + [ATP]_t + K_{MeATP}}{2} - \sqrt{\frac{[Me^{2+}]_t + [ATP]_t + K_{MeATP}}{2}^2 - [Me^{2+}]_t \cdot [ATP]_t} \quad (1)$$

with  $K_{MgATP} = 2.15 \times 10^{-4}$  M (ref. 11) and  $K_{CaATP} = 7.25 \times 10^{-4}$  M (ref. 12, cited from 13).

From the obtained  $[MeATP]$  the concentrations of free ATP and free  $Me^{2+}$  were calculated using

$$[Me^{2+}] = [Me^{2+}]_t - [MeATP] \quad (2)$$

$$\text{and} \quad [ATP] = [ATP]_t - [MeATP]. \quad (3)$$

From these values the reaction rates for constant  $[MeATP]$  at varying  $[Me^{2+}]$  (as shown in Figs 1–3, 6, 8) and for constant  $[Me^{2+}]$  at varying  $[MeATP]$  (Figs 5,7) were interpolated.



Dieses Werk wurde im Jahr 2013 vom Verlag Zeitschrift für Naturforschung in Zusammenarbeit mit der Max-Planck-Gesellschaft zur Förderung der Wissenschaften e.V. digitalisiert und unter folgender Lizenz veröffentlicht: Creative Commons Namensnennung-Keine Bearbeitung 3.0 Deutschland Lizenz.

Zum 01.01.2015 ist eine Anpassung der Lizenzbedingungen (Entfall der Creative Commons Lizenzbedingung „Keine Bearbeitung“) beabsichtigt, um eine Nachnutzung auch im Rahmen zukünftiger wissenschaftlicher Nutzungsformen zu ermöglichen.

This work has been digitized and published in 2013 by Verlag Zeitschrift für Naturforschung in cooperation with the Max Planck Society for the Advancement of Science under a Creative Commons Attribution-NoDerivs 3.0 Germany License.

On 01.01.2015 it is planned to change the License Conditions (the removal of the Creative Commons License condition "no derivative works"). This is to allow reuse in the area of future scientific usage.

### Derivation of the rate equation for the reaction

The derivation of the rate equation was performed on the basis of a rapid equilibrium reaction according to models presented by Botts and Morales<sup>14</sup>, Laidler<sup>15</sup>, Ohlenbusch<sup>16</sup>, and Cleland<sup>17</sup>.

### Chemicals

ATP was obtained from Boehringer, Mannheim, Germany. All other chemicals were purchased from E. Merck, Darmstadt, Germany, and were of reagent grade.

### Results

The reaction rates at various but constant concentrations of MgATP and  $H^+$ -ions are plotted as a function of pMg (Figs 1–3). These figures show that the  $Mg^{2+}$ -ions activate the *E. coli* ATPase at low concentrations and inhibit the enzyme at higher concentrations. The optima of the obtained  $v$ –pMg-functions are shifted to higher metal concentrations with increasing substrate concentration and with increasing hydrogen ion concentration.

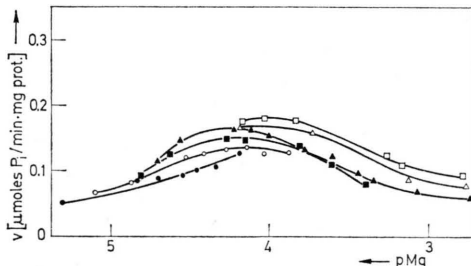


Fig. 1. Plot of  $v$  vs pMg at different constant MgATP-concentrations. ATPase from *E. coli* B 163. 100 mM Tris-HCl-buffer, pH 7.5. [MgATP]:  $\bullet = 35.0 \mu M$ ;  $\circ = 59.5 \mu M$ ;  $\blacktriangledown = 98.0 \mu M$ ;  $\blacktriangle = 134.5 \mu M$ ;  $\square = 220.0 \mu M$ .

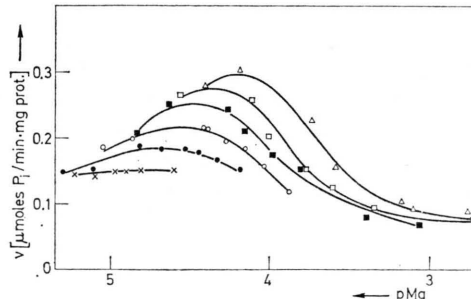


Fig. 2. Plot of  $v$  vs pMg at different constant MgATP-concentrations. ATPase from *E. coli* B 163; 100 mM Tris-HCl-buffer, pH 8.2. [MgATP]:  $\times = 14.3 \mu M$ ;  $\bullet = 35.0 \mu M$ ;  $\circ = 59.5 \mu M$ ;  $\blacksquare = 98.0 \mu M$ ;  $\square = 134.5 \mu M$ ;  $\triangle = 220.0 \mu M$ .

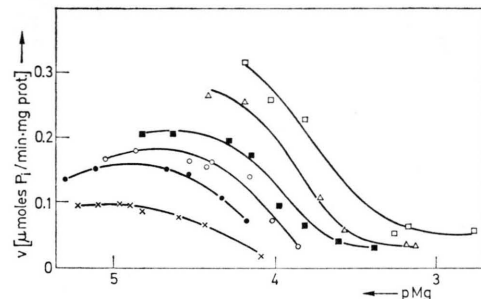


Fig. 3. Plot of  $v$  vs pMg at different constant MgATP-concentrations. ATPase from *E. coli* B 163. 100 mM Tris-HCl-buffer, pH 9.1. [MgATP]:  $\times = 14.3 \mu M$ ;  $\bullet = 35.0 \mu M$ ;  $\circ = 59.5 \mu M$ ;  $\blacksquare = 98.0 \mu M$ ;  $\triangle = 220.0 \mu M$ ;  $\square = 354.0 \mu M$ .

From the values in the ascending parts of the curves in Fig. 1  $1/v = f(1/[Mg^{2+}])$  at constant [MgATP] and  $1/v = f(1/[MgATP])$  at constant  $[Mg^{2+}]$  have been plotted (Figs 4 and 5). Within experimental error the obtained straight lines have

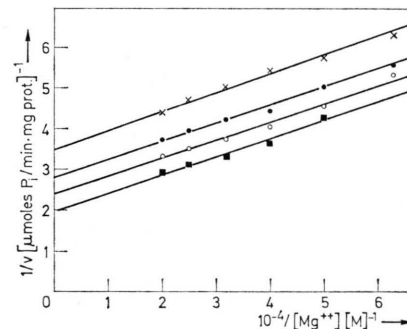


Fig. 4. Plot of  $1/v$  vs  $1/[Mg^{2+}]$  at different MgATP-concentrations. The various values were taken from the ascending part of the curves in Fig. 1. 100 mM Tris-HCl-buffer, pH 7.5. [MgATP]:  $\times = 35.0 \mu M$ ;  $\bullet = 59.5 \mu M$ ;  $\circ = 98.0 \mu M$ ;  $\blacksquare = 220.0 \mu M$ .

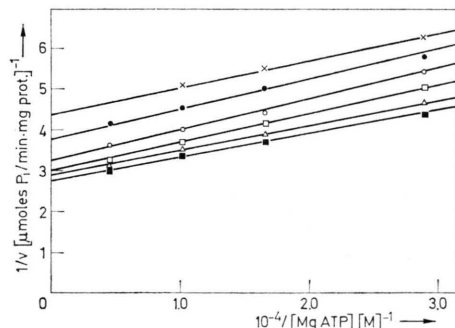


Fig. 5. Plot of  $1/v$  vs  $1/[MgATP]$  at various constant  $Mg^{2+}$ -concentrations. The various values were taken from the ascending part of the curves in Fig. 1. 100 mM Tris-HCl-buffer, pH 7.5. pMg:  $\times = 4.8$ ;  $\bullet = 4.7$ ;  $\circ = 4.6$ ;  $\blacksquare = 4.5$ ;  $\triangle = 4.4$ ;  $\blacksquare = 4.3$ .

a common point of intersection on the abscissa or in the third quadrant. From the values of the descending parts of the curves in Figs 1–3  $1/v$  was plotted against  $[Mg^{2+}]$  at constant  $[MgATP]$  (e.g. Fig. 6) and  $1/v$  against  $1/[MgATP]$  at constant  $[Mg^{2+}]$  (e.g. Fig. 7). We obtained straight lines

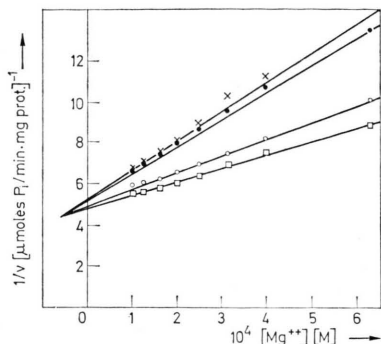


Fig. 6. Plot of  $1/v$  vs  $[Mg^{2+}]$  at various constant  $MgATP$ -concentrations. The various values were taken from the descending part of the curves in Fig. 1. 100 mM Tris-HCl-buffer, pH 7.5.  $[MgATP]$ :  $\times = 98.0 \mu M$ ;  $\bullet = 134.5 \mu M$ ;  $\circ = 223.0 \mu M$ ;  $\square = 350.0 \mu M$ .

with a common point of intersection on the ordinate ( $1/v$  vs  $1/[S]$ ) or in the second quadrant ( $1/v$  vs  $[Mg^{2+}]$ ). With  $Ca^{2+}$  instead of  $Mg^{2+}$  corresponding results were observed (not shown).

However, the plot  $1/v$  vs  $[Mg^{2+}]$  at pH 9.1 was not linear, but  $1/v$  vs  $[Mg^{2+}]^2$  was linear (Fig. 8). From the slopes, the ordinate values and from the common points of intersections of the straight lines (e.g. Figs 5–8), the kinetic constants  $K_m$ ,  $V$ ,  $K_A$  and  $K_I$  were calculated (Table I).

## Discussion

Since the solubilized and purified enzyme is too unstable for reproducible kinetic measurements and

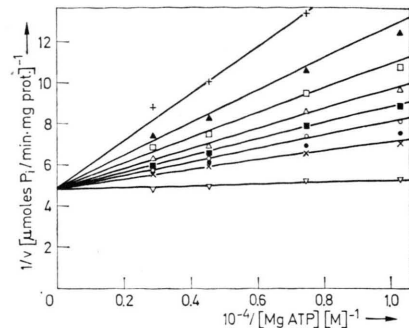


Fig. 7. Plot of  $1/v$  vs  $1/[MgATP]$  at various constant  $Mg^{2+}$ -concentrations. The various values were taken from the descending part of the curves in Fig. 1. 100 mM Tris-HCl-buffer, pH 7.5.  $pMg$ :  $+= 3.2$ ;  $\blacktriangle = 3.4$ ;  $\square = 3.5$ ;  $\triangle = 3.6$ ;  $\blacksquare = 3.7$ ;  $\circ = 3.8$ ;  $\bullet = 3.9$ ;  $\times = 4.0$ .  $\nabla$ :  $[Mg^{2+}] = 0$ ; intercepts with the ordinate from Fig. 6.

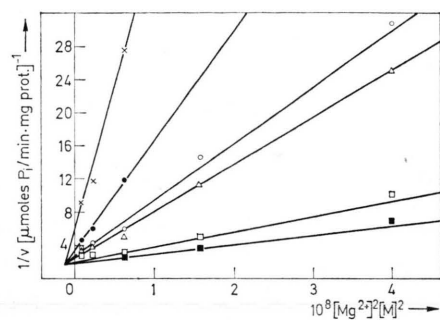


Fig. 8. Plot of  $1/v$  vs  $[Mg^{2+}]^2$  at different constant  $MgATP$ -concentrations. The various values were taken from the descending part of Fig. 3. 100 mM Tris-HCl-buffer, pH 9.1.  $[MgATP]$ :  $\times = 14.3 \mu M$ ;  $\bullet = 35.0 \mu M$ ;  $\circ = 59.5 \mu M$ ;  $\triangle = 98.0 \mu M$ ;  $\square = 223.0 \mu M$ ;  $\blacksquare = 354.0 \mu M$ .

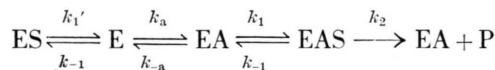
for testing the ATPase-complex in a more physiological state we used the membrane bound enzyme.

The linearity of plots of  $1/v$  vs  $1/[S]$  and  $1/v$  vs

Table I. Kinetic constants for Mg-Ca-ATPase from *E. coli* B 163. Values were taken from  $1/v$  vs  $1/[S]$ ,  $1/v$  vs  $1/[Mg^{2+}]$ ,  $1/v$  vs  $[Mg^{2+}]^2$ . (e.g. Figs 4–8) and from the secondary plots (slopes and ordinate values of Lineweaver-Burk- and Dixon-plots vs effector concentration or  $1/[S]$  resp.).  $K_m$  and  $V$  are real constants ( $[S] \rightarrow \infty$ ,  $[A] \rightarrow \infty$  resp.  $[I] \rightarrow 0$ ).

Substrate	pH	Effector	Acting as	$\frac{V}{\mu\text{mol } P_i}{\text{ min}} \cdot \text{mg prot}}$	$K_m$ [ $\mu M$ ]	$K_A$ [ $\mu M$ ]	$K_I$ [ $\mu M$ ]
MgATP	7.5	$Mg^{2+}$	activator	0.28	20	15	
MgATP	7.5	$Mg^{2+}$	inhibitor	0.21	10		70
MgATP	8.2	$Mg^{2+}$	inhibitor	0.36	12		40
MgATP	9.1	$Mg^{2+}$	inhibitor	0.56	30		35
CaATP	7.5	$Ca^{2+}$	activator	0.16	47	9	
CaATP	9.1	$Ca^{2+}$	inhibitor	0.50	90		64

$1/[A]$  show that one molecule of substrate and one activator ion react per active centre. If there are more ATP-splitting centres within the ATPase complex as probable, they are not interacting. The activator ions are essential for activity. The following model for activation is in agreement with the results:



The substrate molecule can be bound by the free enzyme E and by the enzyme-activator-complex EA. However, only the enzyme-activator-substrate-complex EAS decomposes. This model results in the following reaction rate equation under equilibrium conditions:

$$v = \frac{V \cdot [S]}{\frac{K_m \cdot K_A}{[A]} + \frac{[S] \cdot K_m \cdot K_A}{K_{S'} \cdot [A]} + K_m + [S]} \quad (4)$$

$$K_m = (k_{-1} + k_2)/k_1,$$

$$K_{S'} = k_{-1}'/k_1',$$

$$K_A = k_{-a}/k_a.$$

The features of the straight lines in Figs 4–8 can be seen from the reciprocal form:

$$1/v = 1/V + K_m/V \cdot [S] + \frac{K_A}{V \cdot [A]} (K_m/K_{S'} + K_m/[S]). \quad (5)$$

If substrate and activator are bound independently of each other, straight lines with a common point of intersection on the abscissa appear in the plots of  $1/v = f(1/[S])_A$  and  $1/v = f(1/[A])_S$ .

For  $[S] > K_m$  the quotient  $K_m/[S]$  in Eqn (5) becomes small and the slope of the straight lines in the plots of  $1/v - 1/[A]$  may become independent from  $[S]$ , for  $[A] > K_A$  the slope of the plots  $1/v = f(1/[S])$  becomes independent of  $[A]$ . This has been the case in our experiments. Thus we have obtained straight lines (Figs 4 and 5) which appear to be nearly parallel.

At higher concentrations of divalent cations an inhibition of the *E. coli* ATPase occurs. The common point of intersection of the straight lines on the ordinate in the plot of  $1/v - 1/[S]$  (Fig. 7) and the common point of intersection in the second quadrant

of  $1/v = f([Me^{2+}])$  (Fig. 6) show, that  $Mg^{2+}$  ions are competitive inhibitors with respect to MgATP and  $Ca^{2+}$  ions with respect to CaATP (not shown). Thus  $Me^{2+}$  and  $[MeATP]$  probably compete for the substrate binding centre.

The competitive inhibition of *E. coli* ATPase by divalent metal ions explains the fact that other authors<sup>18–24</sup> obtained higher  $K_m$  values than those reported in Table I. These authors determined the kinetic constants by variation of  $[MgATP]$  or  $[CaATP]$  at constant ratios  $[Me^{2+}]_t/[ATP]_t$  resulting in variable  $Me^{2+}$  concentrations and thus already inhibiting  $Mg^{2+}$  or  $Ca^{2+}$  ion concentrations. Our lower  $K_m$  values agree with the dissociation constant of the “loose” binding site which probably is the catalytic site of mitochondrial  $F_1$ -ATPase<sup>25</sup>. The activation and the competitive inhibition by  $Mg^{2+}$  explain the shift to lower pMg-values and the broadening of the pMg-optima in the  $v$ –pMg-plots with increasing substrate concentrations (Figs 1–3).

In Figs 1–3 a shift of the  $Mg^{2+}$ -optimum to higher values can also be observed by increasing  $H^+$ -ion concentration. This may be explained by a competition between  $Mg^{2+}$  (or  $Ca^{2+}$ ) and  $H^+$  ions for the metal ion binding centre.

There is no qualitative difference between  $Mg^{2+}$  or  $Ca^{2+}$  ions serving as activator. The kinetic constants and the enzyme activity differ somewhat. However, the exact difference between the action of  $Mg^{2+}$  and  $Ca^{2+}$  depends on the accuracy of the dissociation constants of MgATP and CaATP used. As the  $Ca^{2+}$  optima occur at higher concentrations than the  $Mg^{2+}$  optima, the latter metal ions are bound stronger than the  $Ca^{2+}$  ions.

From the dissociation equilibrium for MeATP it follows that varying  $[Me^{2+}]$  at constant  $[MeATP]$  also alters  $[ATP]$ . Therefore the above discussed effects of metal ions on *E. coli* ATPase might be considered being the result of an action of free  $[ATP]$  or of the combined action of  $[Mg^{2+}]$  and  $[ATP]$  as proposed in a recent paper by Skou<sup>26</sup>. The straight lines in Fig. 5 demonstrate that  $[ATP]$  had no influence. On the other hand, when  $1/v - 1/[MgATP]$  is plotted at constant  $[ATP]$  but variable  $[Mg^{2+}]$  (Fig. 9), one should expect straight lines if  $[ATP]$  but not  $[Mg^{2+}]$  influences ATPase activity. However, line [a] at 0.2 mM  $[ATP]$  is curved upwards as a result of the inhibitory effect of  $Mg^{2+}$  ions at high  $Mg^{2+}$  concentrations, [b] at 1.0 mM  $[ATP]$  is curved downwards because in

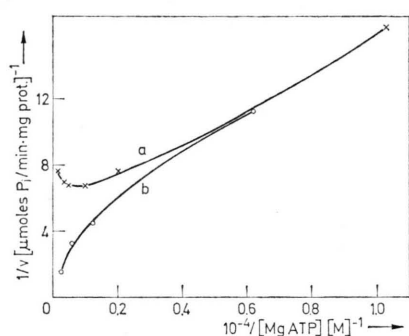


Fig. 9. Plot of  $1/v$  vs  $1/[MgATP]$  at different constant concentrations of free ATP. 100 mM Tris-HCl-buffer, pH 7.5.  
a.  $[ATP] = 0.2$  mM ( $\times$ ); b.  $[ATP] = 1.0$  mM ( $\circ$ ).

this case the metal ion concentrations are lower and activating. Thus these results are in agreement with our assumption that  $Mg^{2+}$  ions and not ATP affects the *E. coli* ATPase.

- <sup>1</sup> G. B. Cox and F. Gibson, *Biochim. Biophys. Acta* **346**, 1–25 [1974].
- <sup>2</sup> W. L. Klein and P. D. Boyer, *J. Biol. Chem.* **247**, 7257–7265 [1972].
- <sup>3</sup> W. Boos, *Ann. Rev. Biochem.* **43**, 123–146 [1974].
- <sup>4</sup> T. Günther, W. Pellnitz, and G. Mariß, *Z. Naturforsch.* **29c**, 54–60 [1974].
- <sup>5</sup> T. Günther and F. Dorn, *Z. Naturforsch.* **21b**, 1076–1081 [1966].
- <sup>6</sup> D. J. Evans, *J. Bacteriol.* **100**, 914–922 [1969].
- <sup>7</sup> C. H. Fiske and Y. Subbarow, *J. Biol. Chem.* **66**, 375–400 [1925].
- <sup>8</sup> J. Lacy, *Analyst* **90**, 65–75 [1965].
- <sup>9</sup> J. Ahlers, *Biochem. J.* **141**, 257–263 [1974].
- <sup>10</sup> O. H. Lowry, N. J. Rosebrough, A. L. Farr, and R. J. Randall, *J. Biol. Chem.* **193**, 265–275 [1951].
- <sup>11</sup> H. U. Wolf and L. Adolph, *Eur. J. Biochem.* **8**, 68–74 [1969].
- <sup>12</sup> L. B. Nanninga, *J. Phys. Chem.* **61**, 1144–1149 [1957].
- <sup>13</sup> L. G. Sillén and A. E. Martell, *Stability Constants of Metal-Ion Complexes*, The Chemical Society, London, Special publication, No. 17, 1964.
- <sup>14</sup> J. Botts and M. Morales, *Trans. Faraday Soc.* **49**, 696–707 [1953].
- <sup>15</sup> K. J. Laidler, *Trans. Faraday Soc.* **52**, 1374–1382 [1956].
- <sup>16</sup> H. D. Ohlenbusch, *Die Kinetik der Wirkung von Effektoren auf stationäre Fermentsysteme*, Springer-Verlag, Berlin 1962.
- <sup>17</sup> W. W. Cleland, *The Enzymes, Kinetics and Mechanism*, P. D. Boyer, ed., **vol. 2**, p. 1, Academic Press, London and New York 1970.
- <sup>18</sup> G. Giordano, C. Riviere, and E. Azoulay, *Biochim. Biophys. Acta* **307**, 513–524 [1973].
- <sup>19</sup> N. Nelson, B. I. Kanner, and D. L. Gutnick, *Proc. Nat. Acad. Sci. U.S.* **71**, 2720–2724 [1974].
- <sup>20</sup> M. Futai, P. C. Sternweis, and L. A. Heppel, *Proc. Nat. Acad. Sci. U.S.* **71**, 2725–2729 [1974].
- <sup>21</sup> R. Farias, L. Londero, and R. E. Trucco, *J. Bacteriol.* **109**, 471–473 [1972].
- <sup>22</sup> H. Kobayashi and Y. Anraku, *J. Biochem.* **71**, 387–399 [1972].
- <sup>23</sup> H. Kobayashi and Y. Anraku, *J. Biokem.* **71**, 387–399 772–781 [1973].
- <sup>24</sup> M.-P. Roisin and A. Kepes, *Biochim. Biophys. Acta* **275**, 333–346 [1972].
- <sup>25</sup> D. A. Hilborn and G. G. Hammes, *Biochemistry* **12**, 983–990 [1973].
- <sup>26</sup> J. C. Skou, *Biochim. Biophys. Acta* **339**, 246–257 [1974].
- <sup>27</sup> T. Günther and F. Dorn, *Z. Naturforsch.* **24b**, 713–717 [1969].
- <sup>28</sup> P. D. Bragg, P. L. Davies, and C. Hou, *Arch. Biochem. Biophys.* **159**, 664–670 [1973].
- <sup>29</sup> N. Nelson, H. Nelson, and E. Racker, *J. Biol. Chem.* **247**, 7657–7662 [1972].
- <sup>30</sup> N. Nelson, D. W. Deters, H. Nelson, and E. Racker, *J. Biol. Chem.* **248**, 2049–2055 [1973].

Plotting  $1/v - 1/[ATP]$  at constant  $[Me^{2+}]$  we obtained curved lines (not shown). On the other hand, plotting  $1/v - 1/[MeATP]$  (Figs 5 and 7) at constant  $[Me^{2+}]$  we obtained straight lines and thus MeATP fulfills Michaelis-Menten kinetics. Thus MeATP and not ATP is the actual substrate.

The competitive inhibition of the Mg-Ca-ATPase activity by  $Mg^{2+}$  which appears at pMg 4 may have biological significance, as the intracellular pMg in *E. coli* cells amounts to 3<sup>27</sup>.

The Mg-Ca-ATPase of *E. coli* consists of subunits<sup>19, 20, 23, 28</sup>. The ATPase-subunits  $\alpha$  and  $\gamma$  have ATPase-activity<sup>29, 30</sup>,  $\delta$  is needed for membrane binding<sup>20</sup>. The  $\epsilon$ -polypeptide could be the ATPase-inhibitor of the complete coupling factor and thus could have a regulatory function<sup>29, 30</sup>. Additionally activation and inhibition of the ATPase by  $Mg^{2+}$  may also have a regulatory effect.